The Scientific Journal of University of Benghazi

www.sjuob.uob.edu.ly

Single Well Petrophysical Analysis: A Case Study of Belle Fourche Shaly-Sand, Hatton Gas Field, Southwest Saskatchewan

Omar M. Derder [1], Mimonitu Opuwari [2]

[1] *Chinook Consulting Services Ltd., 301 14 St NW Suite 306, Calgary, Alberta, T2N 2A1, Canada.*
[2] *Petroleum Geoscience Research Group, University of the Western Cape, Robert Sobukwe Rd, Beliville, Cape Town, 7535, South Africa.*

Received: 09 / 03 / 2021; Accepted: 12 / 07 / 2021

الملخص:

يوجد المكون الصخري بيللي فورشيه بولاية ساسكتشوان في الحوض الرسوبي الغربي في كندا. وقد تكون في العصر الطباشيري، ويتميز بأنه حوض ضحل وقليل السماحية وطبقات متبادلة مختلفة التركيب ودقيقه السمك. حقل هاتون من الدراسات السابقة ينتج ما يعادل 17.24 بليون قدم مكعب من الغاز من البحيرة النفطية سايبروس-ميري فلات.

تتلخص الدراسة للمكون بيللي فورشيه الرملي الطيني باستخدام الطرق الشاملة البتروفيزيائية والجيولوجية. تهدف الدراسة لمعرفة السمك الكلي للمكون وتقييم السمك المنتج فيه ومعرفة الخواص البتروفيزيائية لحجم الطين والمسامية ونسبة التشبع في الحوض باستخدام مسجلات الابار لأشعة الجاما، وتسجيلات الكثافة، وتسجيلات الصوت والمقاومة الكهربائية.

في هذا البحث طوبقت المقاطع الإحصائية مع الدراسات الرسوبية والجيولوجية ودراسة اللب الصخري المحفور من البئر رقم 12-19-13-28W3. تتعدد طرق التحليل والتقويم وكذلك النتائج في هذه الدراسة وذلك لان هذا المكون الطيني يؤثر على تقييم خصائص الحوض لوجود نسب مختلفة من الطين في الحوض وقلة سمكها وتبادلها مع طبقات الرمل المنتجة.

نتائج التحليل بينت ان نسبة عنصر البوتاسيوم ثابته نسبيا رغم زيادة حجم الطين في بعض الأعماق، بينما نسبة الثوريوم تزيد مع زيادة حجم الطين، وكانت نسبة الثوريوم للبوتاسيوم للعينات التي تم دراستها هي 12. ويحتوي الطين على معادن طينية مثل المونتمورلايت وخليط من المعادن الطينية الأخرى. الدراسات العينية اثبتت أيضا زيادة في معدلات عناصر الثوريوم واليورانيوم.

من نتائج الدراسة وجد أن المكون الصخري له سمك يعادل 6.36 متر بينما سمك الطبقة الإنتاجية ا لها سمك يعادل 2.13 متر. الخواص البتروفيزيائية لهذه الدراسة أوضحت ان نسبة متوسط حجم الطين في المكون الصخري 13%، بينما متوسط نسبة المسامية كانت 15% ونسبة التشبع حوالي 43%.

كما ان الدراسة البترفيزيائية مع موجات السرعة الأولية للصوت واستخدام علاقة (قرينبرق-كاستنق) أوضحت أن هناك زيادة خفيفة في سرعة الموجات الصوتية الأولية مع نقص قيمة الكثافة الصخرية لنفس المسافة والعمق التي تم دراسته مما يثبت وجود نسبة تشبع بترولي في الحوض المستهدف دراسته.

هذه الورقة العلمية بينت انه على الرغم من انه تم استخدم الطرق التقليدية باستخدام أجهزة تسجيلات الابار التقليدية وبالطرق الإحصائية الا أنها خرجت بنتائج مهمة ودقيقه مقارنه مع العديد من الدراسات السابقة لنفس المكون الصخري. والدراسة هي تمهيد لدراسة مستقبليه تركز على إيجاد قالب جيولوجي ستاتيكي وديناميكي ومطابقته بالدراسات الهندسية لخصائص المكمن والإنتاج فيه للحصول على تقييم شامل ودقيق.

الكلمات المفتاحية:

الطباشيري العلوي، حوض هاتون الغازي الطيني، الخصائص البتروفيزيائية، القيمة القطعية، المعادن الطينية.

Abstract

This case study shows the petrophysical evaluation of the Belle Fourche Formation, Hatton Gas Field, Southwest Saskatchewan, using conventional well log interpretation techniques. The Belle Fourche reservoir analysed is indicated as shaly-sand formation, while petrophysical parameters calculated includes gross thickness, net thickness, volume of shale, porosity, and water saturation. Cross plots, in conjunction with previous core sedimentology study was used to identify lithology as shale dominated by mixed clay. The potassium content remains relatively constant as the clay content increases. In contrast, the thorium content increases with an increase in the clay content presenting thorium potassium ratio of 12, composed of montmorillonite and mixed-layer clay. Shale content increases as the thorium and uranium content increases. Results from the petrophysical evaluation revealed a gross reservoir thickness of 6.36 m, an average net shaly-sand thickness of 2.13 m, an average volume of clay of 13 %, the porosity of 15 %, and average water saturation of 43 %. Rock petrophysics cross plot of density versus P-wave (Vp) velocity was attempted to identify hydrocarbon saturation. The calculated velocities using the Greenberg and Castagna relation indicate slight increase in Vp and a decrease in density in shaly-sand data indicating hydrocarbon saturation in the reservoir interval. This paper has presented conceptually simple petrophysical method, structured in a manner that is easy to understand for a shaly-sand formation evaluation.

Keywords: Upper Cretaceous, Shaly Gas Reservoir, Low-resistivity, cutoff, Petrophysics.

*Correspondence:

Omar M. Derder
Omar.derder@chinookpetroleum.com

1. INTRODUCTION

Petrophysical evaluation or reservoir characterization generally involves the properties of porous rocks that comprises water saturation, permeability, porosity, permeability, fluid identification, water saturation, and shaliness [1-6]. The integration of rock physics and petrophysics studies, are important in the evaluation of well and field potential [7-9].

The Western Canada Sedimentary Basin (WCSB) contains the majority of Canada's inventory of oil and gas reserves. The Cretaceous reservoir and petrophysical properties in shallow, low permeability, a thin-bedded heterogeneous mudrock succession within the Colorado Group in the WCAB in Alberta, are a prolific self-sourcing tight reservoir [10].

The Belle Fourche Formation (BFF) was defined by [11] in southern Saskatchewan and Alberta. Shallow, low-permeability Cretaceous reservoirs in Saskatchewan have been suggested to contain large un-discovered reserves of biogenic gas [12]. The Medicine Hat-Hatton gas fields straddle the Alberta-Saskatchewan border approximately 75 mi north of the International Boundary (F ig. 1).

Their shallow depths, low permeability, clay-rich sands, and immature, locally generated biogenic gas characterize reservoirs of the Hatton gas field. Despite significant production (>1 MMBbl) from individual wells, unpredictable inflow performance due to anisotropy and fracture dependency has prevented it from being established as a resource play [13].

Within the study field, the recoverable gas is only estimated at 17.24 Bcf from the Cypress-Merryflat Pool. The Cypress/Merryflat Pool reservoir sandstones contain shoreface and lowstand deposits that are progradational, with northwest-southeast shoreline trends, superimposed by a major transgressive surface. In the Bigstick pool, the upper part of BFF is the main reservoir with 2.5 m thick. It characterized by intergranular (primary) porosity, while lower silts (below BFF sand) characterized by micro-porosity (due to high calcite cemented and siderite) interval reveal a second potential reservoir (Fig. 1).

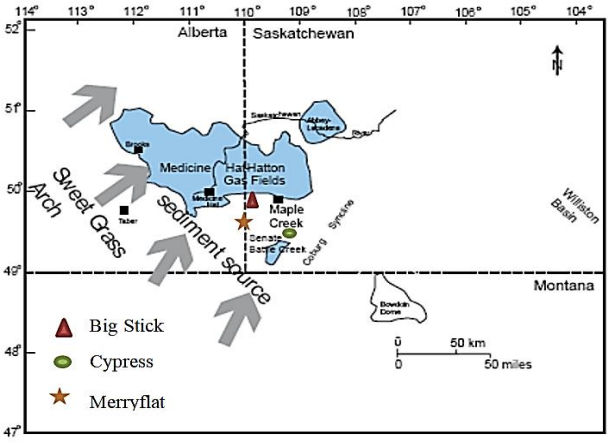


Figure 1. General map of Belle Fourche (Second White Specks sandstone), Hatton Gas Field [11]

An integrated study of the Cretaceous, Belle Fourche sandstone of Lower Colorado Group is presented in this paper. The gas is accommodated in the late Cenomanian-early Turonian sandstone of Second White Specks Sandstone (SWSS), Belle Fourche within Southern Alberta and Saskatchewan (Fig. 2).

In general, the BFF characterizes by thin laminations of very muddy-sandstones, and the sandstone is silty to very fine-grained. The complex reservoir and heterogeneity of the BFF, a standard petrophysical evaluation using conventional logging tools could cause inaccurate reserve estimates. Because of the low permeability and porosity, localized natural fracture networks serve as conduit for the hydrocarbon to flow at economical rates [10].

The petrophysical framework of Cretaceous strata in Saskatchewan and the geological controls on the genesis and distribution of shallow, low-permeability biogenic gas systems are still relatively poorly understood. Some preliminary results are presented in this paper. Shallow gas in south-western Saskatchewan is mainly hosted in low-permeability, fine-grained siliciclastic reservoirs within the BFF is commonly referred to as "Second White Specks sandstones" [14-16].

The main gas producing units in the area are the upper and lower parts of Belle Fourche Formation. A Correlation chart that presents selected Cretaceous rock units from South-eastern Alberta, south-western Saskatchewan, and Montana is shown in (Fig.2). The Belle Fourche formation is middle and late Cenomanian.

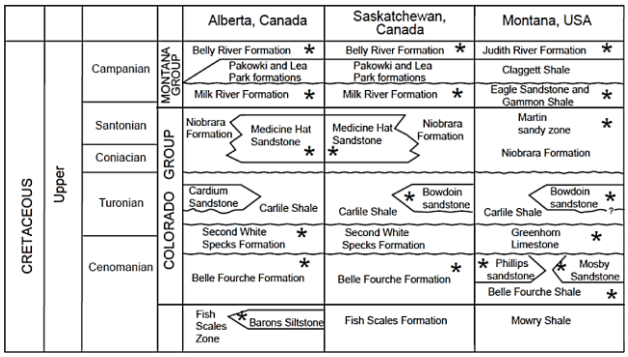


Figure 2. Chart showing stratigraphic column for the Belle Fourche Formation Southern Saskatchewan and Alberta [17].

According to [12], they are mostly unconventional, continuous-type gas accumulations, which are characterized by the overall low permeability and porosity of the reservoir rocks. To address this knowledge gap, a research project has been initiated to re-examine the petrophysical framework and carry out detailed studies of selected shallow gas accumulations.

The purpose of this paper is to evaluate the petrophysical and reservoir parameters of a single well in the Belle Fourche formation. Additionally, to explore the essential petrophysical characteristics that underlie the petrophysical and reservoir properties, discuss the causes for the observed variability.

2. DATA AND METHOD

This study was performed using well log data to calculate petrophysical parameters that include the volume of shale, porosity, and water saturation. The uses of cross plots were adopted in order to provide the lithology information. The available log data used includes raw borehole measurements from the standard wire-line logs recorded in the well are: Natural Gamma log (GR), Natural spectral gamma log (Thorium, Uranium, and Potassium), Caliper log, Density Log,

Bore Hole Compensated Sonic, Litho-Density (RHOB), Compensated Neutron Log (Neutron), and Resistivity logs.

This study shows the results of the interpretation of recorded well logs and data sourced using geoLOGIC's geoSCOUT web portal. Previous work on the selected well 12-19-13-28W3 by Nexen Inc. in the Hatton field, Saskatchewan, gas shale reservoir included developing a digital log database for the wells drilled into the BFF.

Conventional core analyses are rare in the study formation because the zone has not been a primary exploration target. In this well, an 11.84 m core was recovered from 657.85 m to 669.69 m; this core is the source of the only core analyses available in the study area. The paucity of core data limits petrophysical analyses of the BFF because there is a lack of framework, clay mineralogical and the porosity data.

The core data retrieved from the study well was used to identify the lithology and to integrate with the petrophysical data in order to quantify parameters needed to estimate the shale volume, porosity, water saturation and net pay thickness of the BFF.

The evaluation of shaly-sands has a wide variety of procedures. Each of these can result in significantly different reservoir evaluation [18]. However, the shaly formation is probably the most challenging type formation in which to interpret logs such as porosity (Ø) and water saturation (Sw).

The BFF unit in the study well is heterogeneous and complex thin beds. The productive intervals are hard to detect by standard logs. The petrophysical evaluation process is commenced by the evaluation of the shale volume in the formation. The shale volume serves as an input parameter for the determination of other petrophysical parameters.

2.1. The volume of the Shale (Vsh/Vcl)

Shaly-sandstone in reservoirs can be determined from the calculation of the volume of shale in the sand [19]. The volume of shale estimation (Vsh/Vcl) was determined from the GR log. There are various methods existing to calculate the volume of shale, but for the present study, gamma ray log is used because it is one of the best methods [20]. The Gamma-ray index is calculated by using the equation developed by given by Dresser Atlas [21] and Fertl and Frost Jr, [20]. Its mathematical definition is:

$$Volume\ of\ Shale = \frac{GR\ value\ (log) - GR\ (min)}{GR\ (max) - GR\ (min)} \qquad (1)$$

Where:

GR value (log) = GR log value reading of formation to be evaluated [22].

GR (min) = Clean formation

GR (max) = GR value of maximum shale reading in the formation

However, different zones were classified into clean,shaly and shale zones according to [22, 23], as follows:

If Vcl < 10 % = Clean zone.

If Vcl is between 10 to 35 % = Shaly zone

If Vcl > 35 % = Shale zone

The average Vcl calculated in the studied well has an average value of 28 % (Fig.3a) and that of the reservoir interval has an average value of is 13 % (Fig.3b); therefore, the studied formation is interpreted as a shaly-sand formation because the average Vcl is between 10 % and 35 %.

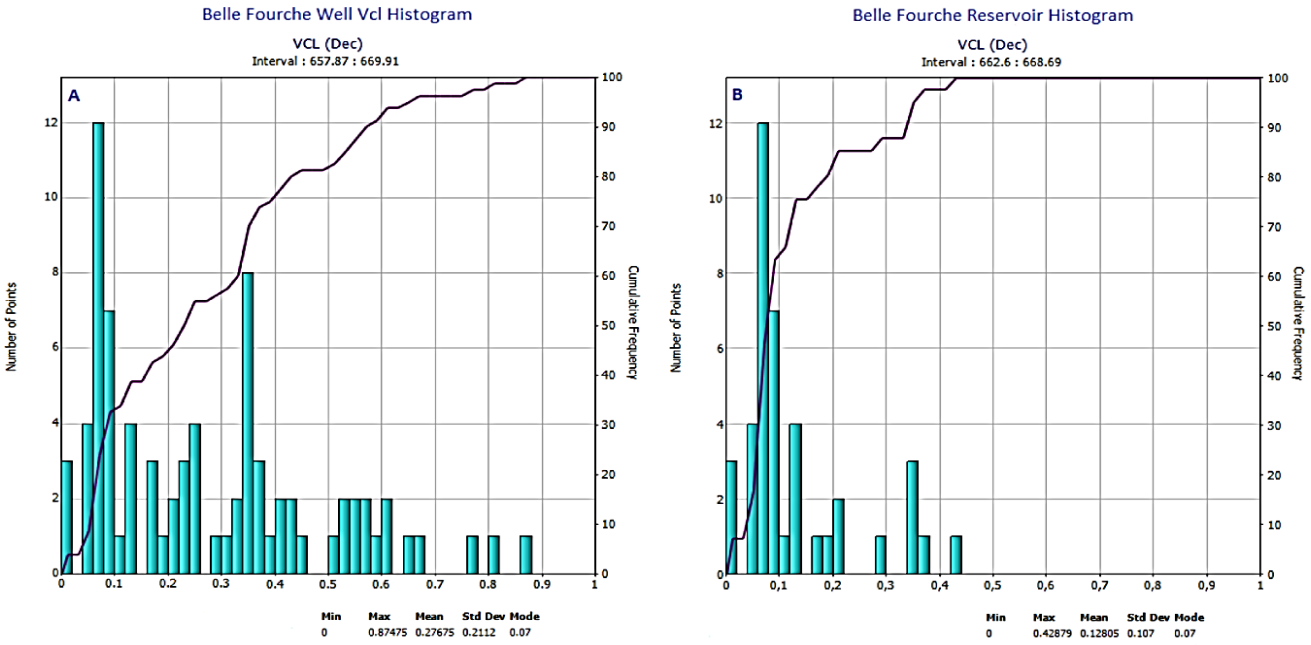


Figure 3. Histogram of **(a)** well volume of clay and **(b)** reservoir volume of clay.

2.2. The Porosity (Ø)

The presence of shale and gas to estimate the porosity is difficult due to various characteristics of shales and gas effect on the responses of the porosity tools. To avoid any misinterpretation of porosity due to gas and shale effects, more than one porosity log is required [24].

The sonic log is not used in this study because of the gas and shale effects, compaction and secondary porosity effects could present in the cemented shaly-sand. Furthermore, the intervals time of the compressional waves over the shales and sands matrix are not provided in this study.

The Neutron logs are used (limestone and sandstones matrix) shows high porosity values. The neutron log might be affected by both free and bound water due to mixed layers of the clay mineral. However, the density log is used to calculate porosity.

To calculate the porosity of rock from log-derived bulk density, it is necessary to know the density of all the individual materials involved, by [19]. The porosity resulting from the density log (ØD) is defined by using the following relationships [25].

$$Porosity\ (ØD) = \frac{\rho ma - \rho b}{\rho ma - \rho f} \qquad (2)$$

Where:

ρma = matrix density (determined from the core)

ρb = bulk density

ρf = fluid density (determined by pressure test)

Density in a shaly formation can be determined by [22]:

$$(ØD\ corr) = \frac{(\rho ma - \rho b) - Vsh\ (\rho ma - \rho sh)}{(\rho ma - \rho f) - (\rho ma - \rho f)} \qquad (3)$$

Where:

ØD corr= corrected density for shale

Vsh = volume of shale

The variation of porosity due to shale present is corrected using the geometrical model. Based on the porosity-clay content relationship, once the fraction of clay volume, c, is less than the porosity, Ø, the clay fractions fit within the sandstone pore space, and the porosity of the mixture, Ø, decrease as fraction of the clay volume increases [26].

2.3. Water Saturation (Sw)

Over the years, various models relating fluid saturation to resistivity have been developed. To determine the water saturation for shaly-sands sequences, the resistivity tool, Array Induction tool is used. The selected interval shows that the geometric form of the existing shale is laminated in the core. The shale has an effect on the porosity calculations.

All models used to calculate Sw are related to clean sandstone model when the volume of shale is significant. Therefore, clean sandstone equation (Archie's equation) will not compensate for clay conductivity; the Sw computation in this study case will be too high.

[27] discussed the correlation between clay volume and the porosity based on well logging data to evaluate the formation of the shaly-sand in Malaysia. This method has been utilized and verifies in this studied case. The ability of mud filtrate to move gas in the invasion zone implies that the formation exhibit permeability to gas. This ability is diagnosed by the difference between flushed zone saturation Sxo, and virgin zone saturation Sw. Sxo is determined in the shaly-sand layer considering that the current shale form is a laminated model.

$$Sxo = \frac{1}{Rxo\sqrt{\frac{Vsh^{\left(1-\frac{Vsh}{2}\right)}}{Rsh} + \frac{ØD\ corr}{aRmf}}} \qquad (4)$$

Where:

Rxo, is water resistivity in the flush zone (obtained from AIT10)

Vsh, shale volume

ØD corr= corrected density for shale

Rsh, Resistivity in shale zone,

a, Tortuosity factor (assumed as 1)

Rmf, the resistivity of mud filtrate (Estimated from mud resistivity as an average of range 0.66 to 1.5

The corrections of shaly-sand model all incline to decrease the water saturation comparative to that be calculated if the shale effect is overlooked in evaluation processes [28]. The core of the well displayed that the geometric form of the prevailing shale is laminated. Therefore, the equation is used to calculate water saturation in this thin shaly-sand case is defined as:

$$Sw = \frac{1}{Rt\sqrt{\frac{Vsh^{\left(1-\frac{Vsh}{2}\right)}}{Rsh} + \frac{ØD\ corr}{aRw}}} \qquad (5)$$

Where:

Rt, the true resistivity of the virgin zone

Rw, the formation water resistivity

Finally, the hydrocarbon saturation Sh is determined as:

$$Sh = 1 - Sw \qquad (6)$$

Formation water resistivity is obtained from the CWLS data. The average value of data from the chart is taken for the closest five wells to the studied well and corrected to the 22°C.

3. RESULTS AND DISCUSSION

The results are presented in three subheadings, which are core description, lithology determination with cross plots and log interpretation.

3.1. Core Description

The core shows that the BFF is a sequence of muddy, very fine sandstone-and intercalated siltstones. The very fine sandstones of high reservoir quality are characterized by upward-coarsening of sand and progressive downward increase in the portion of intercalated siltstone and mudstone, bioturbation, shells traces, and concretionary siderite (Figs. 4a, b, c and d).



Figure 4. Core photographs of the study area. (**a**) Dark-grey calcareous shale & mudstone. (**b**) A uniform, greyish-black, non-calcareous shale low angle ripples interbedded with very fine sand & intercalated siltstone laminations. The coarsening-upward sequences form the main reservoir in the upper part of the BF. (**c**) Shaly silt with calcite cemented in the lower portion of the BF. (**d**) A sharp contact separates the cemented shaly-sand with dark shale. Bioturbation increases of the shale traces are hard to see at the bottom.

Lithology Determinations and Cross Plots

It is a good practice to determine the mineralogy in a formation before performing log analysis because the mineralogical association in rocks has an impact on the interpretation of well logs [29]. Cross plots provide useful information on the lithology and segregate shaly-sand from shale units. These cross plots (Gamma-ray versus Neutron, Gamma-ray versus Density, and Neutron versus Density) provides a qualitative view of the formation lithology content (Figs.5-7).

The Gamma ray versus Neutron cross plot (Fig. 5) depicts the variation in lithology of the studied well. The point of lower GR (< 140 API) and Neutron (< 0.36) indicates shaly-sand units and the points of higher GR (> 140 API) and Neutron (> 0.36) indicates shaly units. The Gamma ray versus grain density (Fig. 6) shows a negative trend between Gamma Ray and Density.

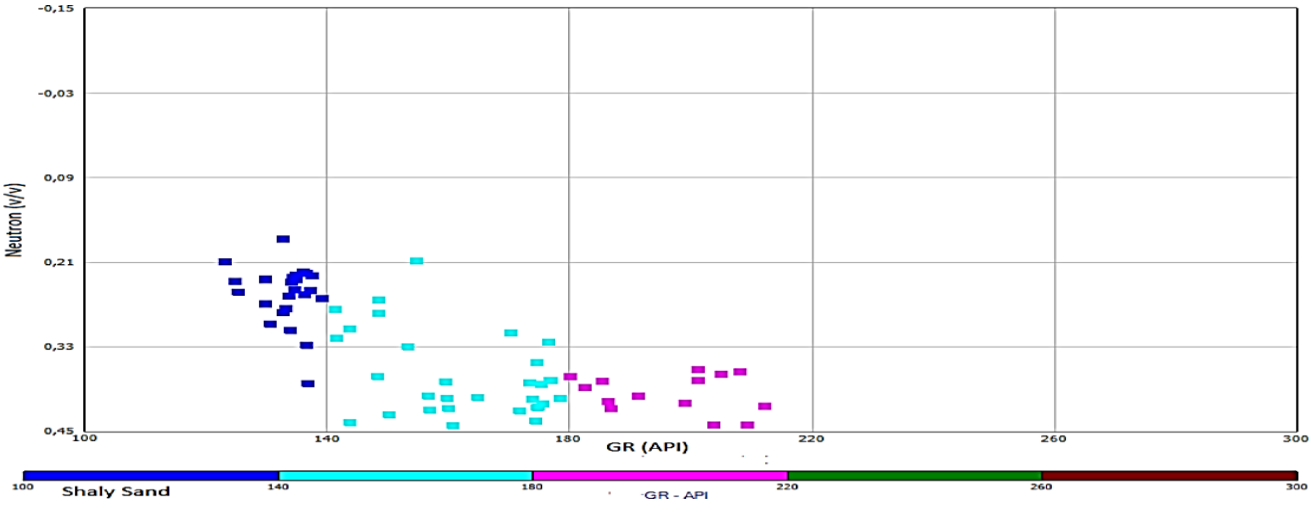


Figure 5: Cross plot of Neutron versus GR log for the identification of lithology.

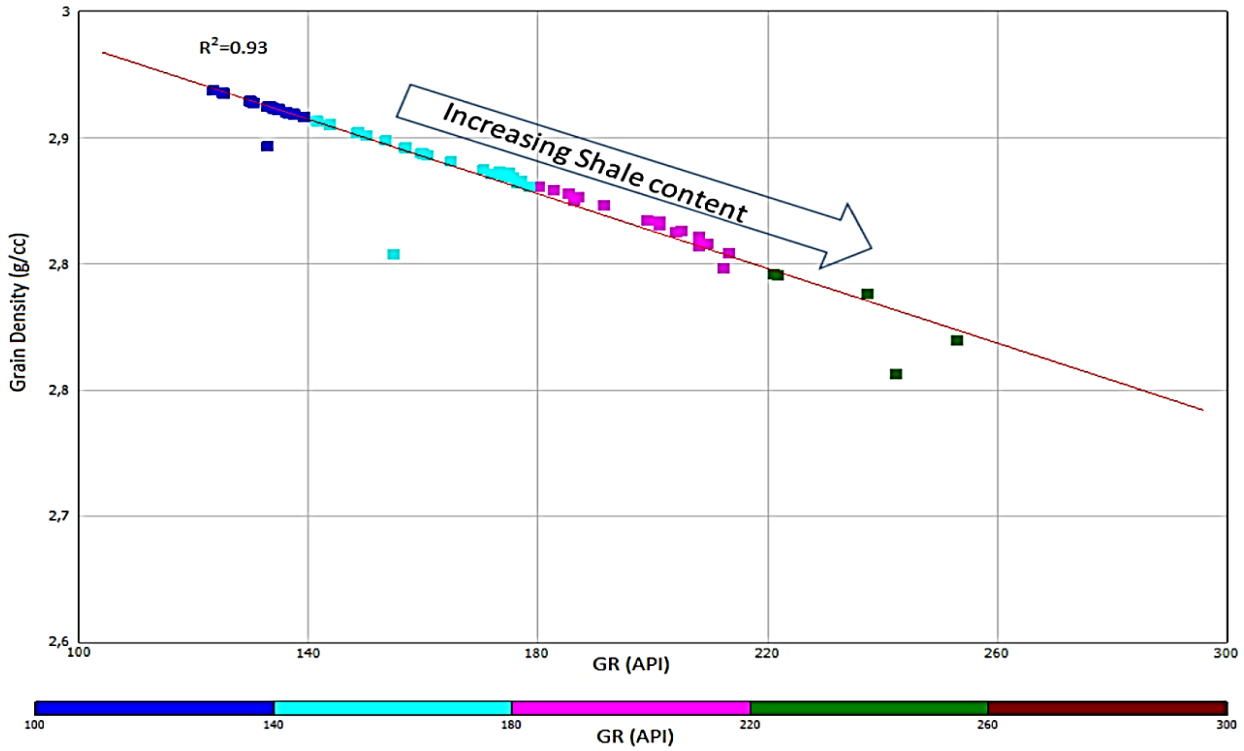


Figure 6: Cross plot of Grain density versus GR log for the identification of lithology.

The neutron versus density, and gamma ray log, a negative trend in the relationship between the two variables was observed (Fig. 7). As the lithology changes from where bentonite layers are recognized, that is, pure shale zone (260 to 140 API, density from 2.46 to 2.75 g/cc, neutron from 0.54 to 0.32 v/v) to shaly-sand zone which is the reservoir (GR < 140 API), a slight change in density (2.75 to 2.70 g/cc) and neutron (0.26 to 0.15 v/v) which might be due to the presence of hydrocarbon. [30] supports our interpretation.

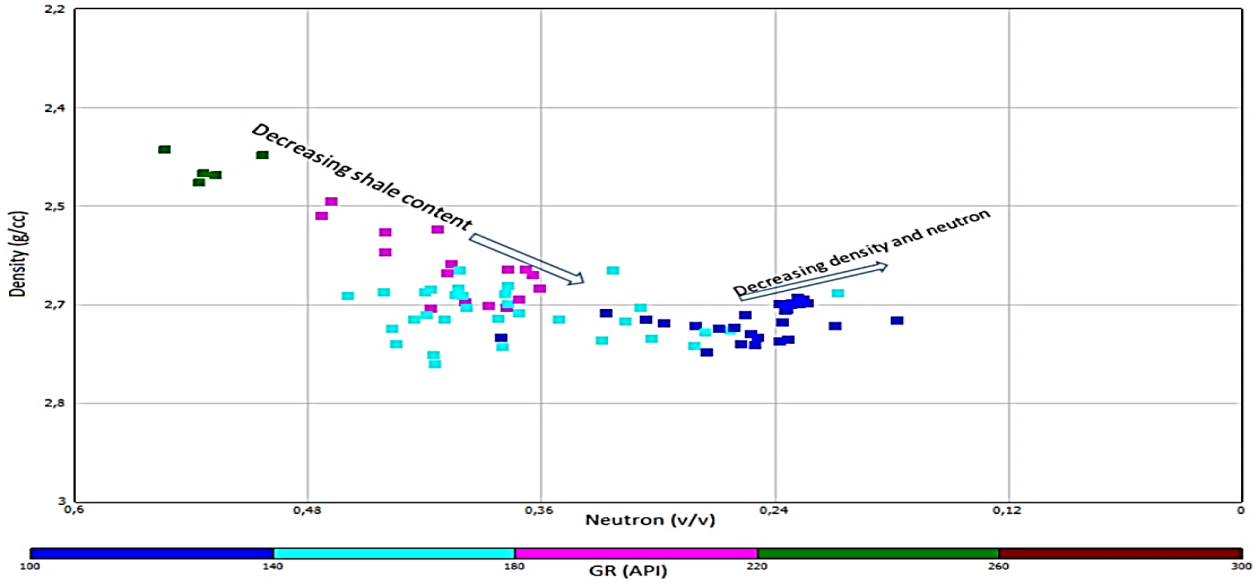


Figure 7: Cross plot of Density (RHOB) versus Neutron log for the identification of lithology.

The natural gamma ray spectrometry logs represent the concentration of thorium, uranium, and potassium in a formation expressed in parts per million (ppm) and potassium is expressed as a percentage. The concentrations of these radioactive elements are shown in (Figs. 8a and b).

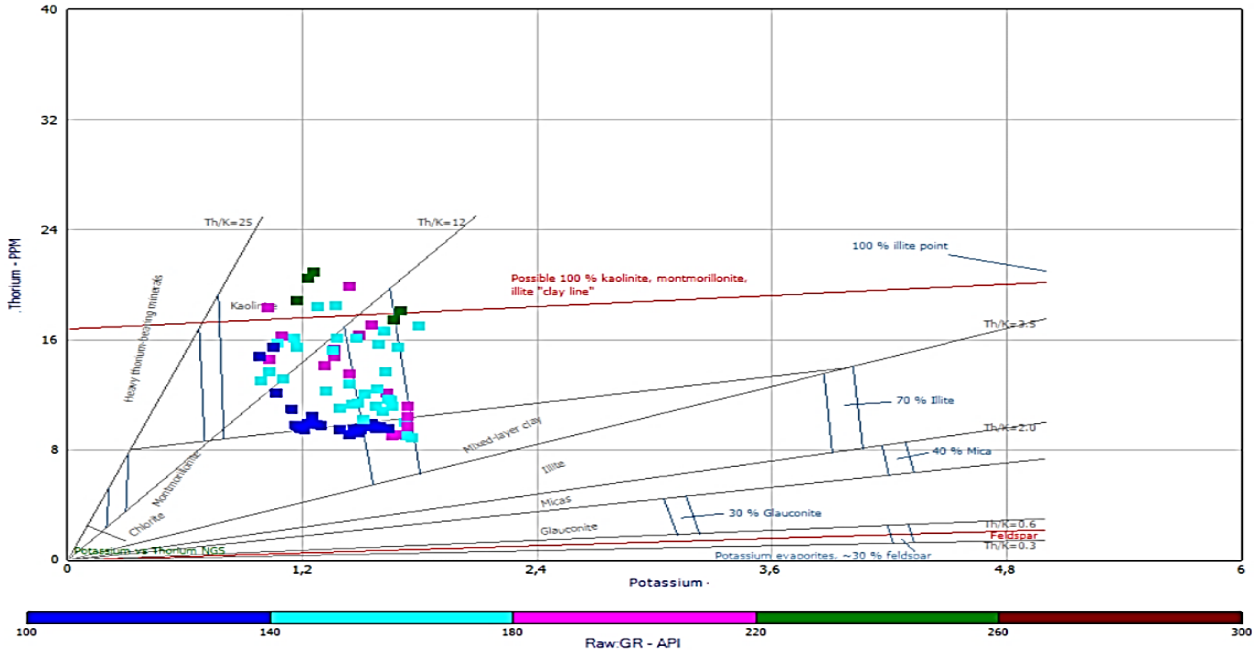


Figure 8a. Cross plot of Thorium Versus Potassium, showing the concentration of mixed clay minerals.

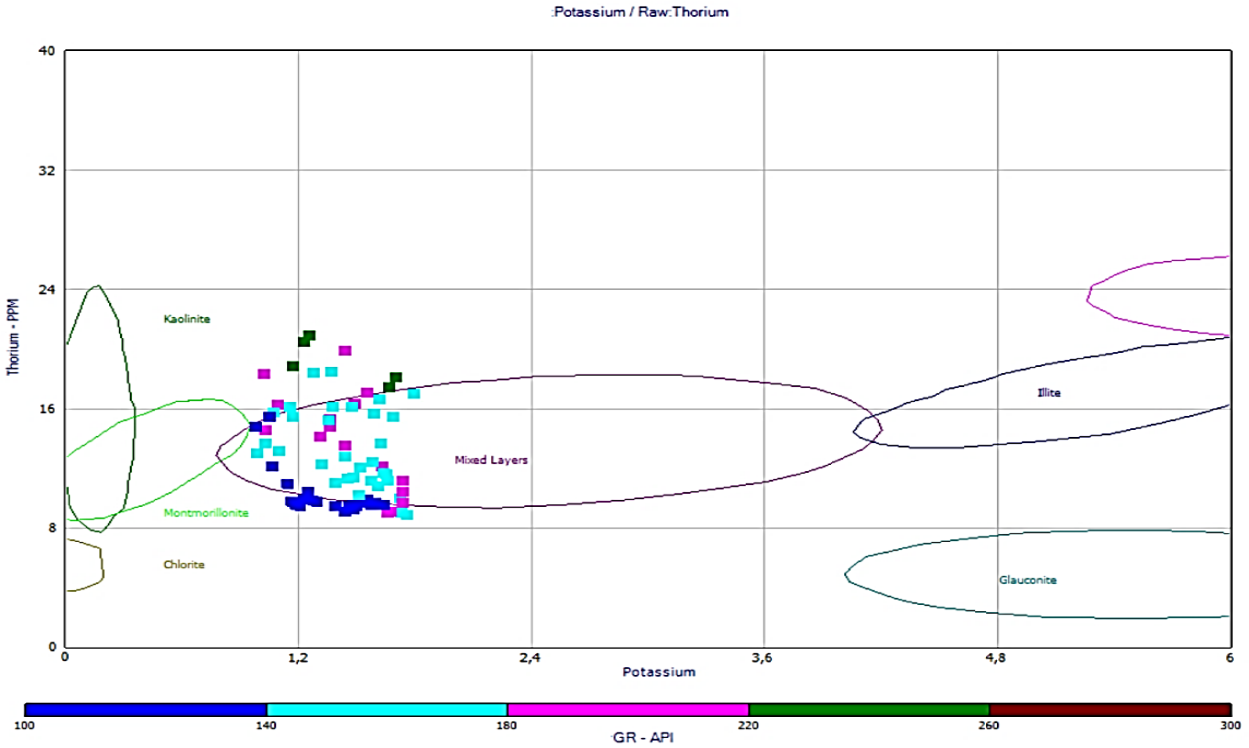


Figure 8b. Cross plot of Thorium Versus Potassium showing the concentration of mixed clay minerals.

The potassium content remains relatively constant as the clay content increases while the thorium content increases with an increase in the clay content presenting thorium potassium ratio of 12, composed of mixed-layer clay. The shale content increases as the thorium and uranium content increases (Fig. 9).

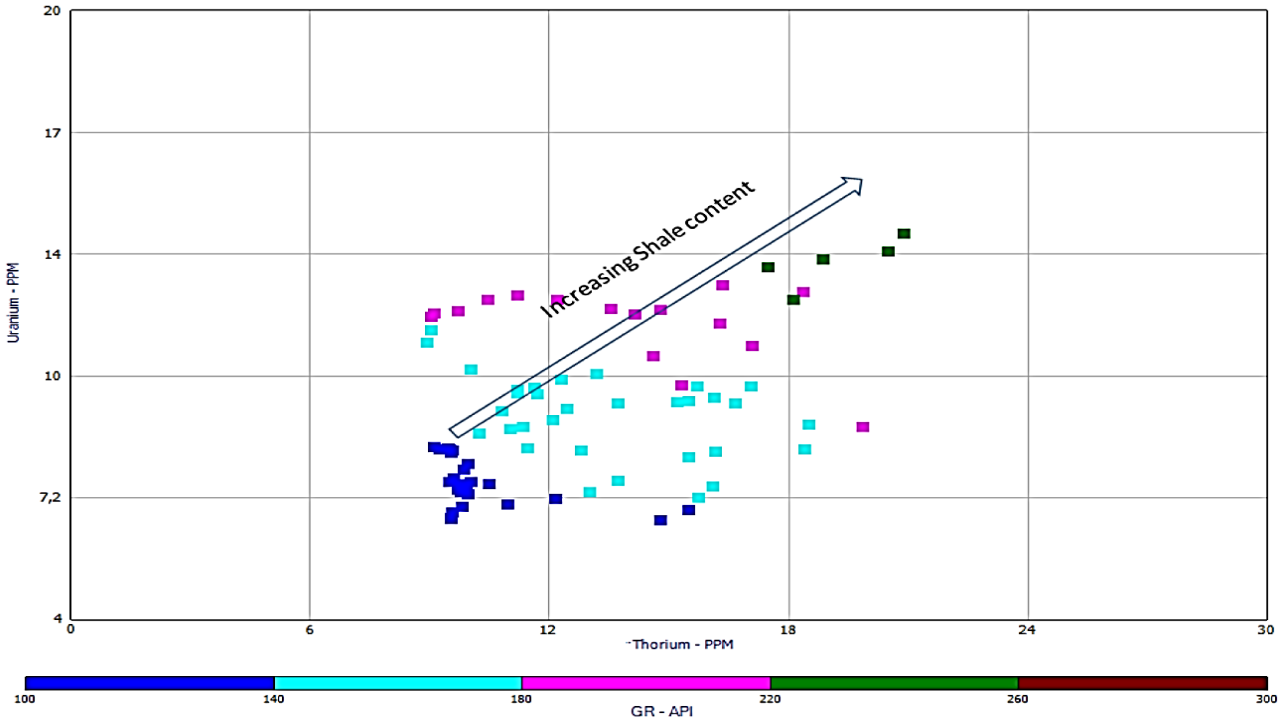


Figure 9. Cross plot of Uranium Versus Thorium indicating increasing shale content as the concentration of uranium and Thorium increases.

The Photoelectric Factor PEF log has been used in the selected interval to record the effective photoelectric absorption cross-section index (Pe) of the formation. The log is used qualitatively to help identify lithology since Pe is matrix specific and unaffected by porosity variations. The log recognizes the shale beds, PEF logs were between 2.7 -3.5 barn/electron (Fig. 10). In samples in which montmorillonite, randomly mixed-layer clays and/or degraded illite are present.

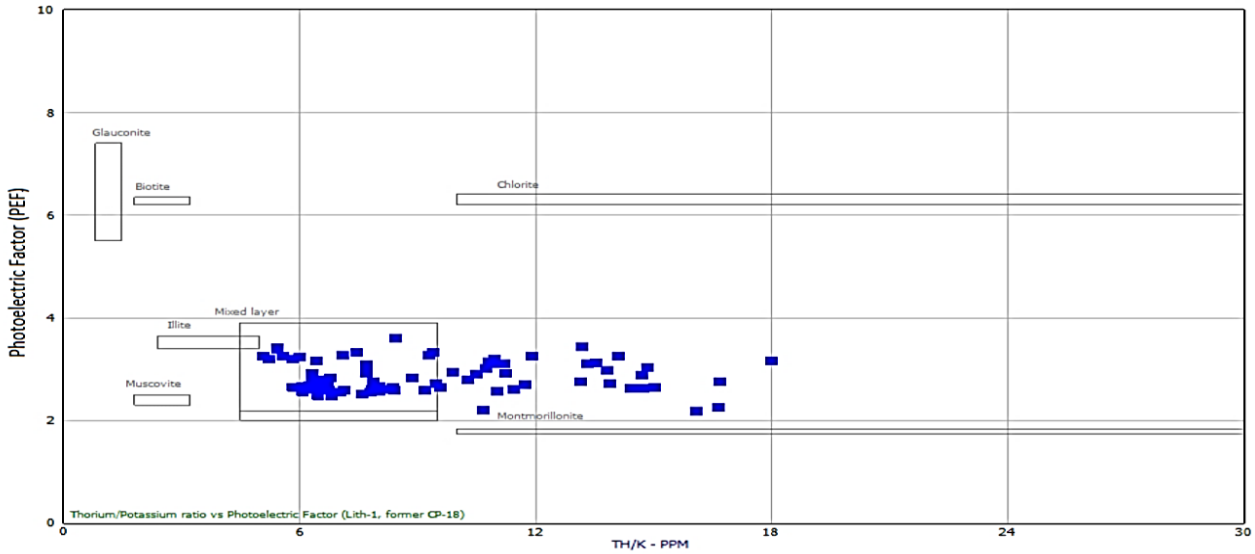


Figure 10. Cross plot of PEF log versus TH/K ratio to identify lithology showing the concentration of mixed clay minerals and montmorillonite.

The grain densities vary from 2428 kg/m3 to 2776 kg/m3, with an average of 2673 kg/m3 for the studied well. The RHOB vary from 2116 kg/m3 to 2483 kg/m3, with an average of 2359 kg/m3 for the studied well.

Rock petrophysics cross plot of grain density versus P-wave (Vp) velocity was attempted to identify hydrocarbon saturation (Fig. 11). The calculated velocities for using the [31] relation, are shown. The result indicates that there is a slight increase in Vp and a decrease in density in the shaly-sand data (blue) indicating hydrocarbon saturation in the reservoir interval.

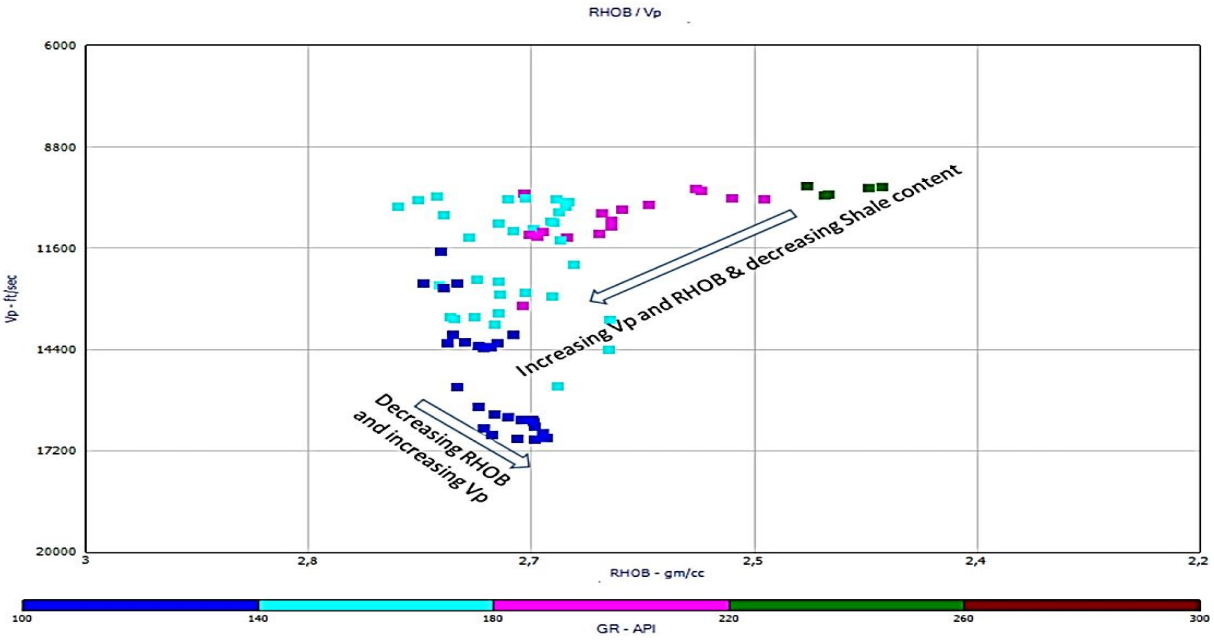


Figure 11. Cross plot of velocity versus grain density indicating a decrease in shale content as Velocity and density increases and appoint of reversal in density as velocity slightly increases

3.2. Log Interpretation

The gamma ray log was used to determine potential reservoir using a baseline of 140 API obtained from the histogram plot presented in (Fig. 12) which means that, deflection of the GR log to the right (> 140 API) represents a shaly unit and GR value < 140 API represents a shaly-sand unit.

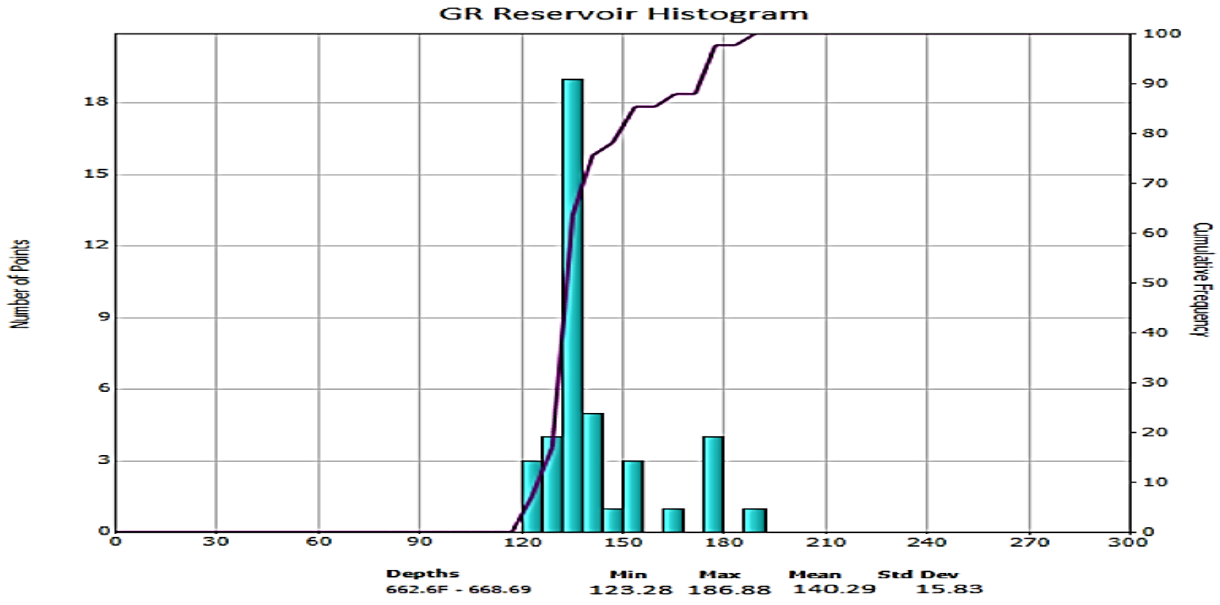


Figure 12. Histogram plot of GR showing limits (minimum, mean and maximum values) used for calculation of the volume of clay.

Based on the criteria set with the GR log, a shaly-sand reservoir was identified at depth 662.6 m to 668.69 m presented in track two of (Fig. 13) using gamma ray log in track 3. Two bentonite beds are detected by gamma ray log considered essential layers for the interpretations. Bentonite beds are located at depths of 664.11 m and 665.26 m with a thickness range of 20 - 30 cm.

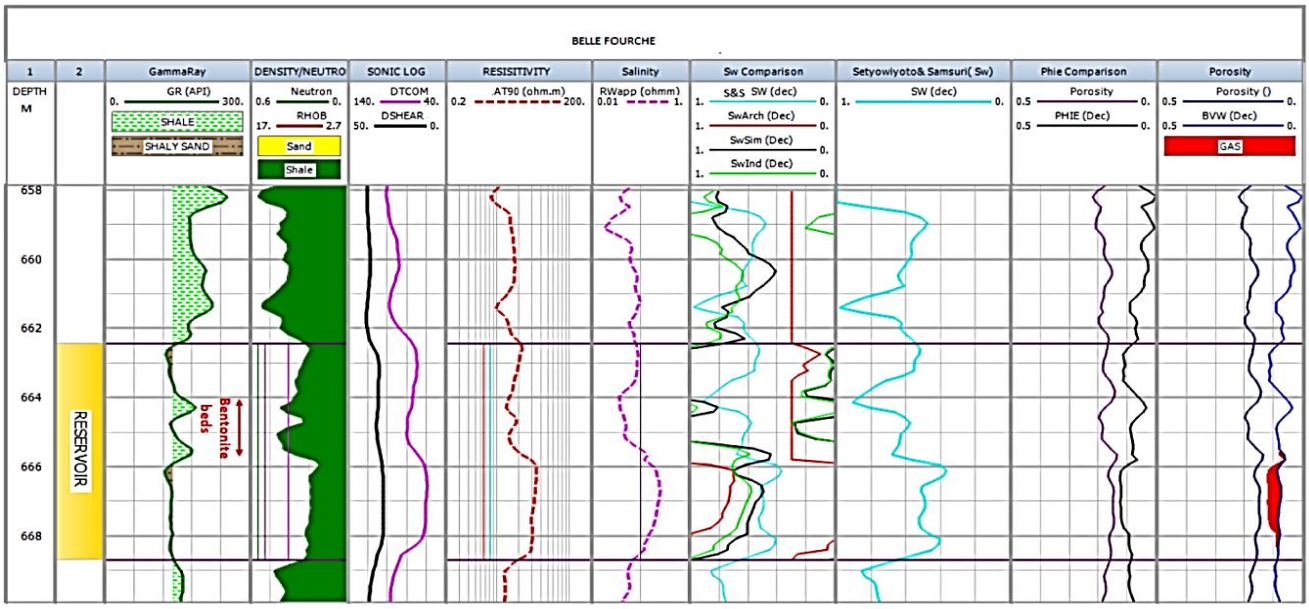


Figure 13. Results of basic log analysis showing reservoir interval and logs used for petrophysical evaluations.

The density-neutron log plotted in track 4 shows shale throughout the interval. The compressional sonic (DTCOM) and shear sonic (DSHEAR) logs in track 5 indicated low values within the reservoir interval; also, the resistivity log in track 6 and the apparent water resistivity showed in track seven both indicated higher resistivity values at the lower part of the reservoir that implies a possible change in fluid saturation.

A comparison of water saturation from the calculated [27] model (S&S Sw), Archie model (SW Archi), Simandoux (Swsim), and Indonesia model (SWInd) presented in track 8. It is evident that the Archie water saturation model could be misleading in a shaly-sand formation due to its erratic curve pattern observed. In contrary, the [27] model presented better and more reliable results in comparison to the other models and was subsequently used to determine water saturation presented in track nine.

A comparison of total porosity and effective porosity model is shown in track 10, presenting a separation between the two variables. At more shaly units, the effective porosity is almost zero, and generally, the effective porosity is less than the total porosity. The bulk volume of water is the product of water saturation, and porosity is used to indicate moveable hydrocarbon plotted in track eleven. This curve shows the presence of hydrocarbon in the lower part of the reservoir.

3.3. Volume of Clay (Vcl)

The volume of clay (Vcl) quantity is defined as the volume of wetted shale per unit volume of reservoir rock [32]. Shaly-sands are sands with a shale component. These shales are a very significant component of shaly-sand reservoirs. The volume of shale needs to be calculated in petrophysical evaluation in order to correct porosity and water saturation results for the little effects of shale. The volume of shale is considered as an indicator for reservoir quality [21]. The result of the volume of clay calculated from equation 1 is presented in track six of (Fig. 14).

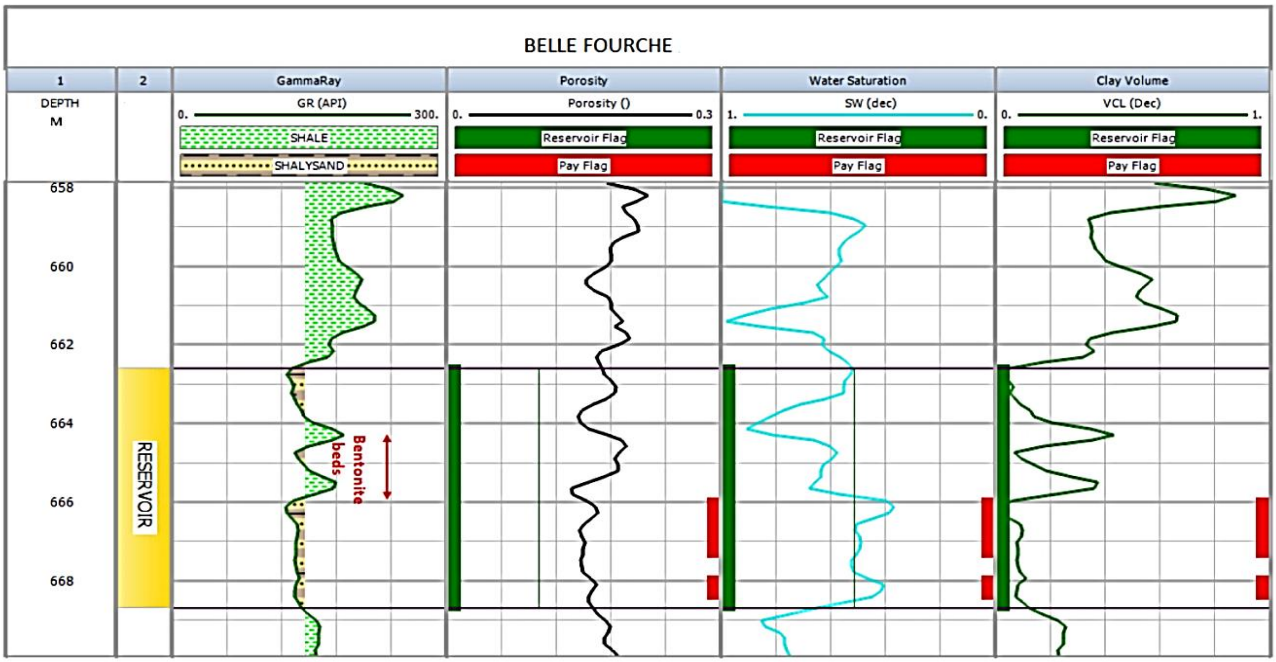


Figure 14. Results of final petrophysical interpretation showing petrophysical properties and gross and net pay flags.

3.4. Porosity Model

The porosity of a rock is regarded as a primary porosity if it is developed during the original sedimentation process by which the rock is created [33]. Processes that synthesize vugs in rocks by groundwater [34, 35]. Generally, porosities incline to be lower in deeper and older rocks due to cementation and overburden pressure stress on the rock creates secondary porosity [36].

Effective porosity (PHIE) is the resultant porosity determined after removal of the effect of clay [18]. However, in an interval of no shale, the total porosity equals the effective porosity. Porosity is the most fundamental hydrocarbon reservoir property [37]. The porosity was calculated from the density log based on equation 6. Presented in track four of (Fig. 14) is the calculated porosity.

The cut-off theory is targeted at defining the useful petrophysical properties of a given geological unit in the presence of poor reservoir zones [29]. There is no single, universally applicable approach to the identification of cut-off off [38]. The assessment of the volume of hydrocarbon requires cut-offs to be defined so that net reservoir intervals (net pay) that contain sufficient hydrocarbon can be identified [39]. The cut-off parameters used in this study are the volume of clay, porosity, and saturation presented in (Figs. 15-16).

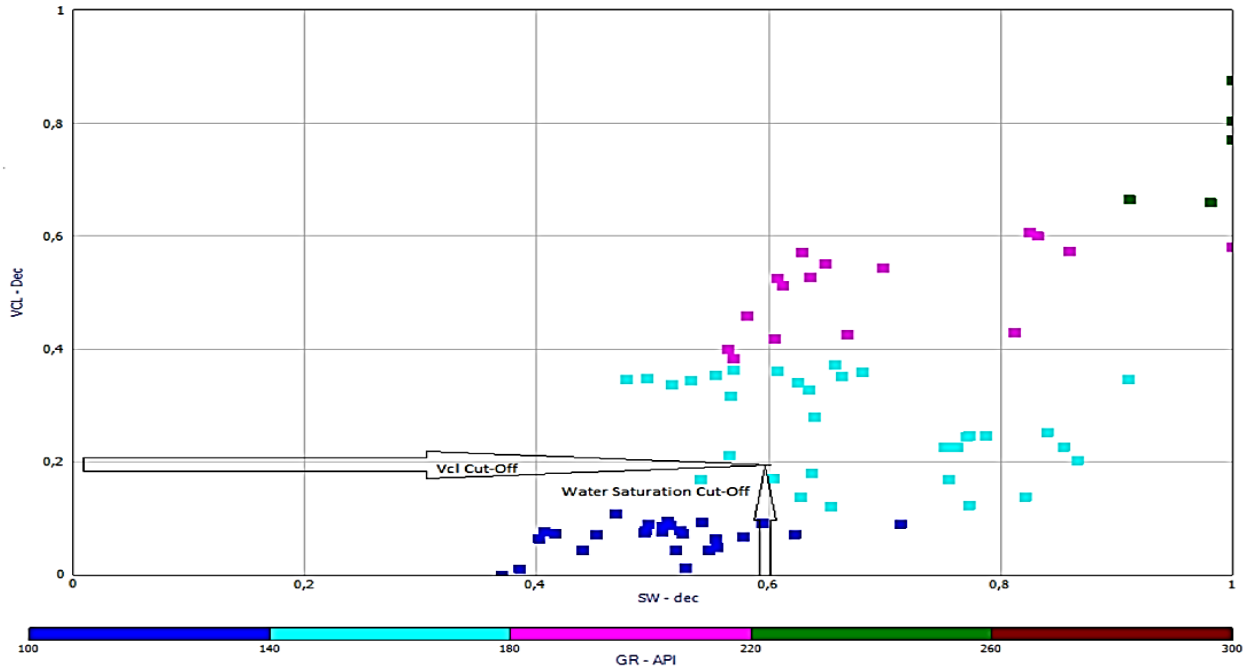


Figure 15: Cross plot of the volume of clay versus water saturation showing cut-off point

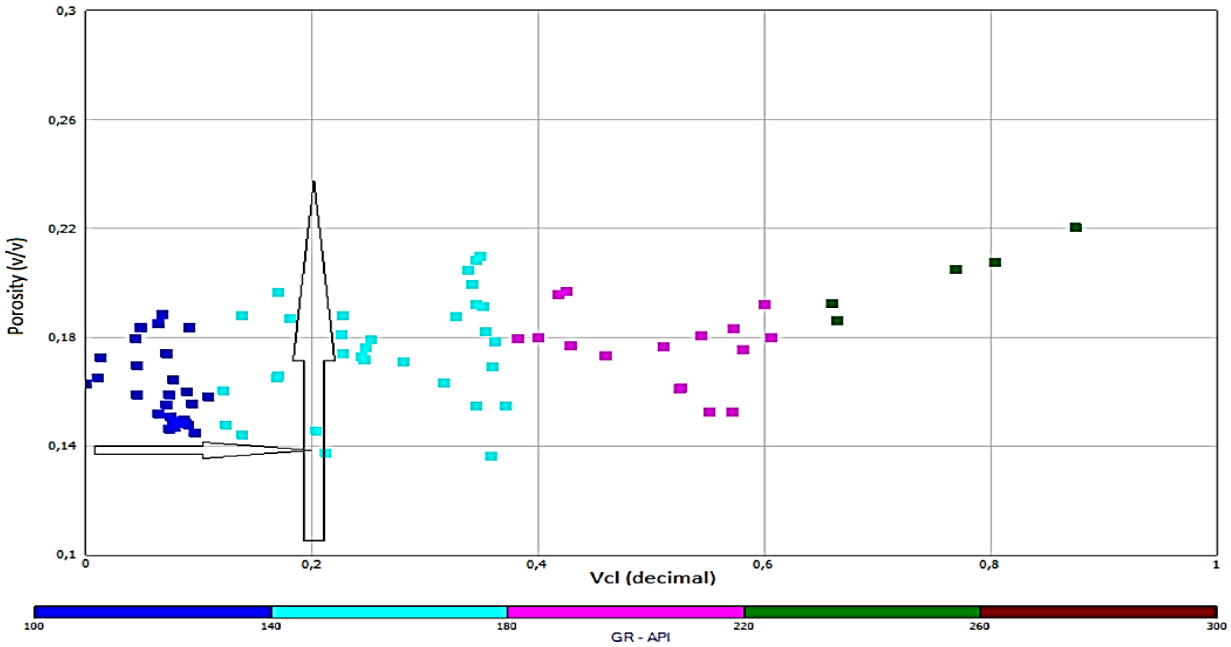


Figure 16: Cross plot of Porosity versus volume of clay showing cut-off points of 14 and 20 percent.

The plot in (Fig. 14) displayed the volume of clay (Vcl) cut-off value for reservoir and non-reservoir rock determined at 0.2. It is interpreted that rocks with a volume of shale/clay value of more than 20 percent was regarded as shale and was not classified as part of the reservoir. In contrary, rocks with a volume of shale values equal to or less than 20 percent are regarded as a reservoir rock. The water saturation cut-off discriminates between hydrocarbon-bearing interval indicated by the pay flag (red) in (Fig. 12) and intervals and water-bearing.

Intervals that have water saturation greater than 55 percent (Fig. 14) is assumed to be non- productive intervals and intervals with water saturation less than 45 percent is assumed to be productive (pay) indicated by red in (Fig. 13). Figure 15 is the cut-off of 14 percent used for the determination of pay and non-productive interval from porosity. That is intervals with

porosity equal to and greater than 14 percent, and volume of shale less 20 percent are grouped as pay (Fig. 16), and intervals with porosity less than 1 percent and volume of clay greater than 20 percent as non-productive.

Choice of cutoffs is made with the help of sensitivity plots showing how averaged parameters vary with a cutoff value and preferably with the help of well-testing data to validate the cut-off choices [40, 41]. Determine the Vcl, porosity and Sw cut-off value depends on the most common or average Vcl, porosity and Sw in the section. Using the cut-off limits, flag curves were created for net reservoir interval (red) and gross reservoir (green) in (Fig. 13). The net to gross ratio is used to calculate the volume of gas initially in place.

The net to gross ratio is used to represent the portion of the reservoir interval that is considered to contribute to the production of hydrocarbon. The concept of the net to gross ratio and cut-off and net pay study is related and has proven useful for reservoir studies. The cut-off parameters used are Vcl ≤ 20 percentages, porosity ≥ 14 %, and water saturation ≤ 55%. The summary Petrophysical average report is presented in Table 1.

The gross shaly- sand reservoir thickness of 6.10 m, net pay thickness of 2.13 m as an interval having the potential to produce hydrocarbon is indicated in Table 1. The result of the petrophysical analysis showed an average volume of clay of 13 percent, porosity of 16 %, and water saturation of 43 percent are calculated.

Table 1. Summary of calculated reservoir pay parameters

Zone	Top Depth (m)	Bottom Depth (m)	Gross Thickness (m)	Net Thickness (m)	Net/Gross Ratio (%)	Average Vcl (%)	Average Porosity (%)	Average Sw (%)
Reservoir	662.6	668.96	6.10	2.13	0.35	13.00	15.50	43.0

4. CONCLUSIONS AND RECOMMENDATIONS

In this study, the petrophysical analysis of the Belle Fourche shaly-sand is presented. Based on the petrophysical interpretation, a shaly-sand reservoir unit is identified at depth 662.6 m to 668.96 m. The reservoir interval has an average net shaly-sand thickness of 2.13 m, an average volume of clay of 13 %, porosity of 15 %, whereas an average water saturation of 43 % was also obtained.

The presence of thin beds characterizes the BFF layers. Most layers show irregular surfaces likely due to soft-sediment deformation or dewatering. Two bentonite beds are detected by gamma ray log considered essential layers for the interpretations. It is a boundary between the BFF and the SWSS. Bentonite beds are located at depths of 664.11 m and 665.26 m with a thickness range of 20 - 30 cm.

Cross plots provide useful information on the lithology and segregate shaly- sand from shale units. The point of lower GR (< 140 API) and Neutron (< 0.36) indicates shaly-sand units and the points of higher GR (> 140 API) and Neutron (> 0.36) indicates shaly units. The cross plot of Neutron versus Density and Gamma ray log shows a negative trend in the relationship between the two variables as the lithology changes from pure shale (high 200 to low 100 API) shaly-sand, which is an increase in density with a corresponding decrease in neutron.

The potassium content remains relatively constant as the clay content increases while the thorium content increases with an increase in the clay content presenting thorium potassium ratio of 12, composed of kaolinite and mixed-layer clay. Shale content increases as the thorium and uranium content increases.

Rock petrophysics cross plot of density versus P-wave (Vp) velocity was attempted to identify hydrocarbon saturation. The calculated velocities for using the Greenberg and Castagna relation indicate that there is a slight increase in Vp and a decrease in density in the shaly-sand data indicating hydrocarbon saturation in the reservoir interval.

More wells, lab data and accurate information such as Rsh, Rxo, Rmf, cementation factor, Rw, Vsh are desired to make this study as reliable for any similar cases. Detailed mineralogical analyses are recommended to verify petrophysical-derived mineralogy.

X-ray diffraction (XRD) and X-ray fluorescence (XRF) on framework and clay minerals is vital key to develop a robust lithological model. Future work should be done to focus on and tie in the static or volumetric models, where the cutoffs are used to evaluate hydrocarbons in place with the dynamic condition (dynamic flow), whereby the static cutoffs are tied to another engineering parameter such as DST, well production tests and relative permeability.

5. ACKNOWLEDGMENTS

The authors express thanks to the University of Calgary, geoLOGIC systems, Canada, for their support and their generous donation of data used in this study. Special thanks are given to my colleague Madi Mazegh for his preliminary review and Synergy Company for the use of Interactive Petrophysics (IP) software package.

6. REFERENCES

1. Mukerji T, Avseth P, Mavko G, Takahashi I, González EF, Statistical rock physics: Combining rock physics, information theory, and geostatistics to reduce uncertainty in seismic reservoir characterization. The Leading Edge, 2001, 20, p 313–319.
2. Omudu LM, Ebeniro JO, Xynogalas M, Osayande N, Olotu S, Fluid discrimination and reservoir characterization from onshore Niger Delta. In SEG Technical Program Expanded Abstracts, 2008; Society Exploration Geophysicists, 2008, p 2001–2005.
3. Inichinbia S, Sule, PO, Ahmed AL, Hamaza H, Lawal KM, Petrophysical analysis of among hydrocarbon field fluid

and lithofacies using well log data. IOSR J Appl Geol Geophys, 2014, 2, 86–96.

4. Singha D, Chatterjee R, Rock physics modeling in sand reservoir through well log analysis, Krishna-Godavari basin, India. Geomechanics and Engineering, 2017, 13, p 99–117.

5. Das B, Chatterjee R, Well log data analysis for lithology and fluid identification in Krishna-Godavari Basin, India. Arabian Journal of Geosciences, 2018, 11, 231.

6. Magoba, M.; Opuwari, M., Petrophysical interpretation and fluid substitution modelling of the upper shallow marine sandstone reservoirs in the Bredasdorp Basin, offshore South Africa. Journal of Petroleum Exploration and Production Technology, 2020, 10, 783–803.

7. Avseth P, Mukerji T, Mavko G, Dvorkin J, Rock-physics diagnostics of depositional texture, diagenetic alterations, and reservoir heterogeneity in high-porosity siliciclastic sediments and rocks—A review of selected models and suggested work flows. Geophysics, 2010, 75, 75A31–75A47.

8. Goodway B, Chen T, Downton J, Improved AVO fluid detection and lithology discrimination using Lamé petrophysical parameters;"λρ","μρ", & "λ/μ fluid stack", from P and S inversions. In SEG Technical Program Expanded Abstracts; Society of Exploration Geophysicists, 1997, 183–186.

9. Khan N, Rehman K, Petrophysical evaluation and fluid substitution modeling for reservoir depiction of Jurassic Datta Formation in the Canada oil field, Khyber Pakhtunkhwa, northwest Pakistan. Journal of Petroleum Exploration and Production Technology, 2019, 9, p 159–176.

10. Marion KP, Integrating Petrophysics and Allostratigraphy to Find Sweet Spots in the Upper Cretaceous Belle Fourche and Second White Specks Alloformations, West-Central Alberta, Canada, 2018,.

11. Bloch J, Schröder-Adams C, Leckie DA, McIntyre DJ, Craig J, Staniland M, Revised stratigraphy of the lower Colorado Group (Albian to Turonian), western Canada. Bulletin of Canadian Petroleum Geology, 1993, 41, 325–348.

12. Shurr GW, Ridgley JL, Unconventional shallow biogenic gas systems. 2002, AAPG bulletin, 86, 1939–1969.

13. MacKay P, Second White Specks Formation: new concepts for understanding fractured reservoirs. American Association of Petroleum Geologists Search & Discovery Article, (Abstract), Playmaker Forum, Calgary, 2014, 27th.

14. Pedersen, P.K., 2004, Shallow gas research project in Southwestern Saskatchewan: Revised lithostratigraphy of the Colorado Group and reservoir architecture of the Belle Fourche and Second White Specks in the Senate Pool. v1, p 1 -15.

15. Tyagi A, Plint, AG, McNeil DH, Correlation of physical surfaces, bentonites, and biozones in the Cretaceous Colorado Group from the Alberta Foothills to southwest Saskatchewan, and a revision of the Belle Fourche-Second White Specks formational boundary. Canadian Journal of Earth Sciences, 2007, 44, 871–888.

16. Furmann, A.; Mastalerz, M.; Bish, D.; Schimmelmann, A.; Pedersen, P.K., 2016, Porosity and pore size distribution in mudrocks from the Belle Fourche and Second White Specks Formations in Alberta, Canada. AAPG Bulletin, 100, 1265–1288.

17. Ridgley JL, Regional Geochemical study of the Upper Cretaceous Shallow Biogenic Gas System in Sasketchewan, Alberta, and Montana-application of isotope and compositional systametics to understanding the distribution of gas resources, 2002, 1, 143-150.

18. Worthington PF, Conjunctive interpretation of core and log data through association of the effective and total porosity models. Geological Society, London, Special Publications, 1998, 136, 213–223.

19. Asquith GB, Gibson, CR, Basic Relationships of Well Log Interpretation, AAPG, Tusla, 1982, 244.

20. Fertl WH, Frost Jr E, Evaluation of shaly clastic reservoir rocks. Journal of Petroleum Technology, 1980, 32, 1–641.

21. Dresser Industries Inc., Dresser Atlas log interpretation charts, Houston, Tex, 1979, 108.

22. Opuwari M, Petrophysical evaluation of the Albian age gas bearing sandstone reservoirs of the OM field, Orange basin, South Africa. PhD Thesis, University of the Western Cape, Cape Town, 2010, 371.

23. Ghorab M, Shazly, T, A Comparative Study Between Pickett's Plot and Xy Cross Plot Methods on Abu Roach Formation at the South Western of Wadi El-Natrun Area, Western Desert, Egypt. Journal of Applied Sciences Research, 2008, 4, 1974–1984.

24. Bassiouni Z, Theory, measurement, and interpretation of well logs; Henry L. Doherty Memorial Fund of AIME, Society of Petroleum Engineers; ISBN 1-55563—056-1, 1st ed, 1994, 4, 373.

25. Wyllie MRJ, The fundamentals of well log interpretation; Academic Press, 3rd New York, 1963, 238.

26. Marion D, Nur A, Alabert F, Modelling The Relationships between Sonic Velocity, Porosity, Permeability, and Shaliness in Sand, Shale, and Shaley Sand. In proceedings of the SPWLA 30th Annual Logging Symposium, Denever, Colorado, 1989,

27. Setyowiyoto J, Samsuri A, Formation evaluation: Correlation between clay volume and porosity based on well logging data. In Proceedings of the scientific conference III-University of Kebangsaan Malaysia; 2008, 1–9.

28. Hamada GM, An Integrated Approach to determine shale volume and hydrocarbon potential in shaly sands in the Gulf of Suez. SPWLA, 1999, 40, No. 3.

29. Cosentino L, Integrated reservoir studies; Editions Technip., 2001, ISBN: 2-7108-0797-1. 336 p.

30. Luthi S, Geological well logs: Their use in reservoir modeling; Springer Science & Business Media, 1st edition, 2001, 373.

31. Greenberg ML, Castagna JP, Shear-wave velocity estimation in porous rocks: theoretical formulation, preliminary verification and applications1. Geophysical prospecting, 1992, 40, 195–209.

32. Katahara K, what is shale to a petrophysicist? The Leading Edge, 2008, 27, issue 6, 738–741.

33. Schmidt V, McDonald DA, The role of secondary porosity in the course of sandstone diagenesis, 1979, 26: 159-174.

34. Asquith GB, Handbook of Log Evaluation Techniques. Methods in Exploration Series, AAPG Publ, Tusla, Okla, 1985, 47p.

35. Crain ER, Log analysis handbook, volume 1: Quantitative log analysis methods, PennWell, Tusla, OK, 1986, 684p.

36. Dutton SP, Diggs TN, Evolution of porosity and permeability in the lower Cretaceous Travis Peak Formation, East Texas. AAPG bulletin, 1992, 76, 252–269.

37. Kuila U, McCarty DK, Derkowski A, Fischer TB, Prasad M, Total porosity measurement in gas shales by the water immersion porosimetry (WIP) method, 2014,117, 1115–1129.

38. Worthington, PF, Cosentino L, The role of cut-offs in integrated reservoir studies. SPE Reservoir Evaluation & Engineering, 2005, 8, 276–290.

39. Cluff SG, Cluff, R.M, Petrophysics of the Lance sandstone reservoirs in Jonah field, Sublette Country, Wyoming, 2004, Chapter 12, 215-241.

40. Derder O, Petrophysical Considerations in Evaluating the Montney Formation (unit c), West-Central area, Alberta, Canada. Reservoir Journal, CSPG, 2015a, 42, Issue 03, 14-18.

41. Derder O, Petrophysical Considerations in Evaluating the Montney Formation (unit c), West-Central area, Alberta, Canada. Reservoir Journal, CSPG, 2015b, 42, Issue 04, 15-19.